Fast 2D Harmonic Filtering of MRI phase; application to discriminating cerebral microbleeds in a multicenter clinical dataset

Takoua Kaaouana[1,2], Ludovic de Rochefort[3], Thomas Samaille[1,2], Nathalie Thierry[4], Genevieve Chene[4], Christine Delmaire[5], Didier Dormont[6], and Marie Chupin[1]

[1]*CRICM, UPMC UMR_S975, INSERM U975, CNRS UMR7225, ICM, INRIA, Paris, France,* [2]*CATI, Paris, France,* [3]*Univ. Paris-Sud, CNRS IR4M UMR8081, Orsay, France,* [4]*U897, INSERM, Bordeaux, France,* [5]*Neuroradiology, CHRU Roger Salengro, Lille, France,* [6]*Neuroradiology, CHRU pitie salpetriere, Paris, France*

INTRODUCTION

Cerebral microbleeds (CMBs) have emerged as a new imaging marker of small vessel diseases, mainly hypertensive vasculopathy and cerebral amyloid angiopathy. They may play a crucial role in degenerative pathology such as Alzheimer's disease [1, 2]. Composed of hemosiderin, CMBs can be efficiently detected with MRI sequences sensitive to magnetic susceptibility (e.g. gradient recalled echo T2*W images). Nevertheless, identification remains challenging because of confounding structures and lesions. In fact, most T2*W hyposignals result from local magnetic field inhomogeneity and can be identified either as CMBs, veins or brain micro-calcifications (BMCs). Differential diagnosis of paramagnetic CMBs and diamagnetic BMCs requires an additional CT scan. Quantitative susceptibility mapping techniques were proposed to discriminate between diamagnetic and paramagnetic structures [3], but they require a full 3D dataset and complex post-processing. Raw phase map analysis has been proposed but detection is limited due to background effects and phase wrapping [4]. Here, we propose an enhanced detection using fast 2D phase processing including unwrapping and harmonic filtering applicable on multicenter data acquired in standardized clinical settings to discriminate between CMBs and BMCs.

MATERIAL

Experiments were performed on 28 patients with CMBs from the multicenter MEMENTO cohort. T2W multi-slice 2D GRE sequences from Siemens (14 datasets) and Philips (14 datasets) 3T systems were used to acquire 2.5mm thick axial slices of the brain, with 1mm×1mm in plane resolution and TR/TE/FA=650ms/20ms/20°. Reconstruction matrix was 240×240×65 on Philips systems and 256×256×70 on Siemens systems, covering the whole brain with anisotropic resolution.

METHODS

To filter out background effects from the field, we used a 2D approximation of harmonic filtering [5, 6]. The field inside the brain, B, can be decomposed as the sum of internal variations, Bin, and variations induced by external sources, Bout. From Maxwell equations, the external field is harmonic inside the brain ($\Delta B_{out}=0$) and $\Delta B=\Delta B_{in}$. Here, to isolate local variations, a harmonic 2D filter was used (**Fig.1**). Slice-by-slice phase unwrapping was performed by forcing the point by point difference between$]-\pi, \pi]$ when calculating the gradients, and the divergence was then calculated to get ΔB. The Laplacian was set to 0 outside a mask generated with SPM imposing proper boundary conditions. Integration to recover B_{in} was then done in Fourier domain using a regularized inverse 2D Laplace filter (Tikhonov regularization, parameter set to 0.002). If $\Delta = k_x^2 + k_y^2$ denotes the discrete Laplace operator used, the inverse was $\Delta_{reg}^{-1} = (k_x^2 + k_y^2)/[(k_x^2 + k_y^2)^2 + \alpha^2]$.

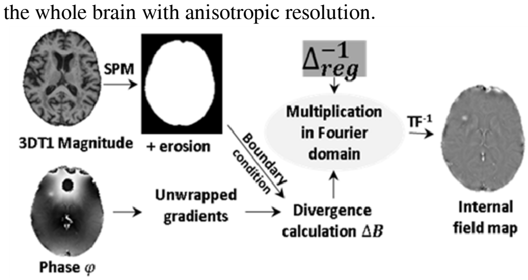

Fig. 1 Schematic illustration of 2D harmonic filtering

RESULTS

Phase wraps were efficiently removed. 2D Harmonic filter (2DHF) removes background effects and preserves local phase variation. SPM masking prior to integration allows limiting artifacts at brain boundaries.

- ***Comparison of 2DHF with projection onto dipole fields on clinical data***

Comparison of 2DHF with the "projection onto dipole fields" (PDF) method [3, 7] was performed. 2DHF was approximately 100 times faster than PDF (for 512 iterations). PDF and 2DHF induced similar results; a good visibility of deep gray matter nuclei and blood vessels was observed, and similar contrast was noted between CMBs and their surroundings using both methods. However, sagittal slices demonstrate that, unlike PDF, 2DHF removes the slice-by-slice phase artifact visible in the data (**Fig.2**).

- ***Differentiation between CMBs and BMCs***

Both CMBs and mimicking BMCs are dot-like susceptibility inclusions, that can be detected on the magnitude image and that create dipole-like patterns in the internal field map (**Fig.3**). For paramagnetic inclusions such as CMBs, dipolar effect is seen as ring-like structure with a sign inversion (- + -), whereas it is (+ - +) for diamagnetic inclusions such as BMCs or the calcified choroid plexus shown in (**Fig.4**).

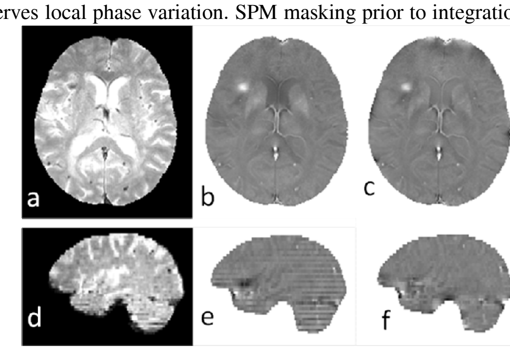

Fig. 2 Acquired 2D dataset, with CMBs, is shown in an axial section in the top row and a sagittal section in bottom row, with the magnitude image (a) and (d), the PDF internal field map (b) and (e), the 2DHF internal field map (c) and (f).

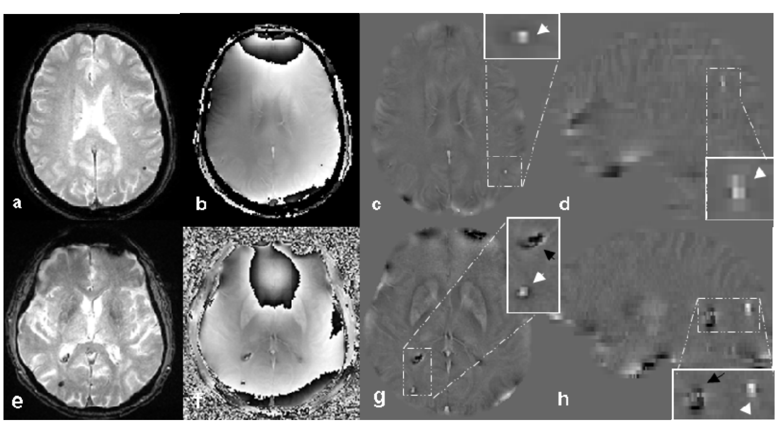

Fig. 3 Philips (a,b,c,d) and Siemens (e,f,g,h) sample cases. Magnitude image (a,e), native phase image (b,f), and internal field map; axial (c,g) and sagittal (d,h). Zoom in white rectangle showing a dipolar pattern CMB (white arrow) and a physiologic calcification of the choroid plexus (black arrow).

DICUSSION AND CONCLUSION

Phase wraps and background effects were efficiently removed. Resulting internal field maps have successfully characterized CMBs as paramagnetic dipole patterns. Sophisticated techniques proposed in the literature, such as PDF, are very time consuming and the precision needed highly depends on the targeted application. The internal field map obtained using 2DHF may provide an efficient tool for clinicians for an enhanced detection of CMBs and to discriminate them from BMCs. Its fast processing proved robust on phase images from 2D T2* clinical acquisitions.

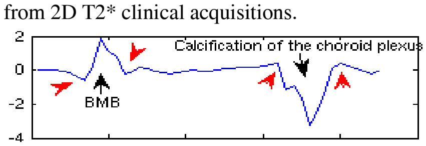

Fig. 4 Sign inversion for either side of CMB and the calcification.

REFERENCES 1. Greenberg S, et al. Neurology 2009, 8(2):165:174. 2. C. Cordonnier and W M, Van Der Flier, Brain 2011, 134 (2) 335:344,. 3. de Rochefort et al. MRM 2010 63:194. 3. 4.Yamada et al., Radiology 1996, 198:171. 5. de Rochefort et al. ISMRM 2010 4997. 6. Schweser et al., NeuroImage 2011, 54 (4) 2789 :2807. 7. Liu et al. NMR in Biomedicine, 24(9):1129-1136, 2011.